



Stable isotope potential of Northern Vietnam stalagmites: A 51-cave survey with the Hendy test and U/Th analysis

Duong Thuy Nguyen¹, Dung Chi Nguyen^{2*}, Thuy Thi An², Chun-Yuan Huang^{3,4}, Chuan-Chou Shen^{3,4}, Czuppon György⁵, Dong Van Bui⁶, Linh Ngoc Nguyen⁶, Hong-Wei Chiang⁷, Yue-Gau Chen⁷, Ha Vu Van², Quang Minh Nguyen², Tuan Minh Dang², Lam Dinh Doan², Ben Marwick⁸, Yin Lin²

¹*VNU Vietnam Japan University, Hanoi, Vietnam*

²*Institute of Earth Sciences, VAST, Hanoi, Vietnam*

³*High-Precision Mass Spectrometry and Environment Change Laboratory (HISPEC), Department of Geosciences, National Taiwan University, Taipei 10617, Taiwan, ROC*

⁴*Research Center for Future Earth, National Taiwan University, Taipei 10617, Taiwan, ROC*

⁵*Institute for Geological and Geochemical Research, HUN-REN Research Centre for Astronomy and Earth Sciences, Budapest, Hungary*

⁶*VNU University of Science, Hanoi, Vietnam*

⁷*Research Center for Environmental Changes, Academia Sinica, Taipei, 11529, Taiwan, ROC*

⁸*Department of Anthropology, University of Washington, Seattle, 98195, Washington, USA*

Received 09 August 2025; Received in revised form 08 December 2025; Accepted 31 December 2025

ABSTRACT

Northern Vietnam's karst landscapes offer an untapped potential for paleo-monsoon research, complementing the extensive speleothem records of Southwest China. Here, we surveyed 51 caves across seven provinces, targeting those with humidity exceeding 95% from 2017 to 2024, and collected 127 broken stalagmites to evaluate their stable-isotope potential ($\delta^{18}\text{O}$, $\delta^{13}\text{C}$) as paleoclimate proxies. Focusing on caves in Hoa Binh and nearby karst-rich regions, we applied Hendy tests to 56 subsamples of eight layers on four stalagmites, NS3, HS3, HS7, and HS16, to assess the isotopic equilibrium conditions. The deposition intervals of the four stalagmites, determined using U/Th dating, range from 36 to 60 thousand years ago (ka). Small 1-sigma variations of $\pm 0.04\text{--}0.20\text{\textperthousand}$ in coeval $\delta^{18}\text{O}$ values across all eight layers suggest deposition under near oxygen isotope equilibrium. Combined with fast growth rates exceeding 0.09 mm/year, this evidence suggests high-resolution potential for paleohydroclimate reconstruction using stalagmite $\delta^{18}\text{O}$ data. However, one-sigma variations of $\pm 0.04\text{--}0.71\text{\textperthousand}$ of coeval $\delta^{13}\text{C}$ data reflect relatively large carbon isotopic fractionation during the degassing process. It suggests that stalagmite $\delta^{13}\text{C}$ records from these caves should be carefully evaluated before use in paleoclimate reconstructions.

Keywords: Northern Vietnam, stalagmites, Oxygen isotope, Hendy test, Paleoclimate proxy.

1. Introduction

Stalagmites from Southeast Asia likely preserve $\delta^{18}\text{O}$ as a proxy for rainfall amount

and moisture-source shifts, reflecting monsoon intensity, while $\delta^{13}\text{C}$ tracks vegetation changes and soil CO_2 dynamics, providing a broader paleoenvironmental context (Genty et al., 2003; Yang et al., 2016;

*Corresponding author, Email: ncdung@ies.vast.vn

Dorale et al., 1992). Globally, speleothem records demonstrate their versatility: European stalagmites capture glacial-interglacial transitions (Genty et al., 2003), Brazilian records reveal South American Monsoon variability (Cruz et al., 2005), and Indian stalagmites document Holocene monsoon fluctuations (Sinha et al., 2005). In Asia, China's high-resolution records correlate $\delta^{18}\text{O}$ values with East Asian Monsoon strength, validated by equilibrium deposition under near-saturated humidity ($> 95\%$) (Wang et al., 2001; Cheng et al., 2013; Dykoski et al., 2005). With its comparable karst geology and humid conditions, Northern Vietnam holds similar promise for paleoclimate reconstruction (Ford & Williams, 2010; Henderson, 2006). Previous studies in Vietnam, such as Nguyen et al. (2020) and Nguyen et al. (2022), analyzed speleothems from a single cave (Thuong Thien) and identified monsoon signals spanning more than 30 kyr, linked to Heinrich Event 3 and D-O events 2–4. However, these efforts lack the regional scope necessary to fully integrate Southeast Asia into the broader monsoon framework, a gap this study aims to address (Chiang et al., 2020; Wolf et al., 2023).

Northern Vietnam's karst belt, encompassing provinces such as Hoa Binh, Son La, and Lai Chau, hosts numerous caves with stalagmites formed under high-humidity conditions that are conducive to isotopic preservation (Ford & Williams, 2010; Henderson, 2006). Unlike China's extensively studied caves, Vietnam's speleothem potential remains largely untapped, with few systematic surveys or multi-site analyses conducted to date (Nguyen et al., 2020; 2022; Chiang et al., 2025). Positioned near the Intertropical Convergence Zone (ITCZ) and influenced by moisture from the East Vietnam Sea, this region can capture distinct monsoon signals, enhancing the spatial context of China's

northern datasets (Chiang et al., 2025; Yang et al., 2016). For instance, China's records show $\delta^{18}\text{O}$ ranges of -9 to -6‰ during monsoon peaks (Dykoski et al., 2005; Cheng et al., 2016), while data from Northern Vietnam suggest similar variability (Nguyen et al., 2020; 2022). Furthermore, during glacial periods when our samples formed (36–60 ka), the exposure of the East Sea shelf fundamentally altered regional atmospheric circulation, affecting Vietnam differently than southern China, providing a complementary perspective on glacial-age tropical circulation (Hanebuth et al., 2006). Yet, challenges such as the aragonite-to-calcite transformation and porosity observed in less humid caves highlight the need for careful site selection (Fairchild et al., 2006; McDermott, 2004).

This study draws on global speleothem research to explore the untapped potential of Northern Vietnam as a paleoclimate archive (Hendy, 1971; Genty et al., 2003). Our objectives are threefold: first, to identify caves and stalagmites suitable for paleoclimate research through extensive surveying and rigorous testing; second, to establish a methodological framework for Northern Vietnam speleothem studies, surpassing the scale of prior efforts; and third, to explore the preliminary potential of isotopic proxies for monsoon reconstruction, laying the groundwork for future high-resolution analyses. While capable of contributing to late Quaternary monsoon studies potentially linked to glacial forcing or ITCZ shifts (Chiang et al., 2025; Yang et al., 2016) this pilot study establishes a foundation rather than a comprehensive reconstruction (Ford & Williams, 2010; Henderson, 2006). Ongoing isotopic work will build on these findings to enhance our understanding of Southeast Asian paleoclimate (Dorale et al., 2007; Genty et al., 2003).

2. Regional setting

2.1. Location

Northern Vietnam encompasses the provinces situated north of Thanh Hoa. It includes both lowland and mountainous regions (Fig. 1). The region's cave systems are predominantly located within the northern mountainous provinces, including Lao Cai, Yen Bai, Dien Bien, Hoa Binh, Lai Chau, Son La, Ha Giang, Cao Bang, Bac Kan, Lang Son, Tuyen Quang, Thai Nguyen, Phu Tho, Quang Ninh, and Ninh Binh. Between 2017 and 2024, this study conducted field expeditions to 51 caves across Lao Cai, Dien Bien, Hoa Binh, Lai Chau, Son La, Ha Giang, Cao Bang, Bac Kan, Lang Son, and Ninh Binh for the collection of stalagmites for paleoclimatic analysis (Table 1, Fig. 1).

2.2. Geological settings

Northern Vietnam has common carbonate formations divided into four main groups (The Department of Geology and Minerals of Vietnam, 2005; Tran Van Tri, 2009):

(i) Precambrian and Cambrian carbonate formations are distributed in the Lao Cai, Ha Giang, Tuyen Quang, and Yen Bai areas. The main components are marble, limestone, clayish limestone, and black limestone.

(ii) Devonian carbonate formations are mainly distributed in the northeastern region: Ha Giang, Tuyen Quang, and Cao Bang. The main components are thin- to medium-bedded limestone, cherty limestone, clayey limestone, and thick-bedded to massive limestone.

(iii) Carboniferous Permian carbonate formations are widely distributed throughout the northern region, including Ha Giang, Cao Bang, Lang Son, and Quang Ninh. The main components are light-gray, thick limestone blocks and black, thin limestone blocks.

(iv) Triassic carbonate formations are mainly distributed in the Northwest region, forming a narrow strip extending in the Northwest-Southeast direction from Lai Chau, Dien Bien, Son La, Hoa Binh, Ninh Binh, and Thanh Hoa. The rocks mainly comprise limestone, cherty, massive, and dolomitized limestone.

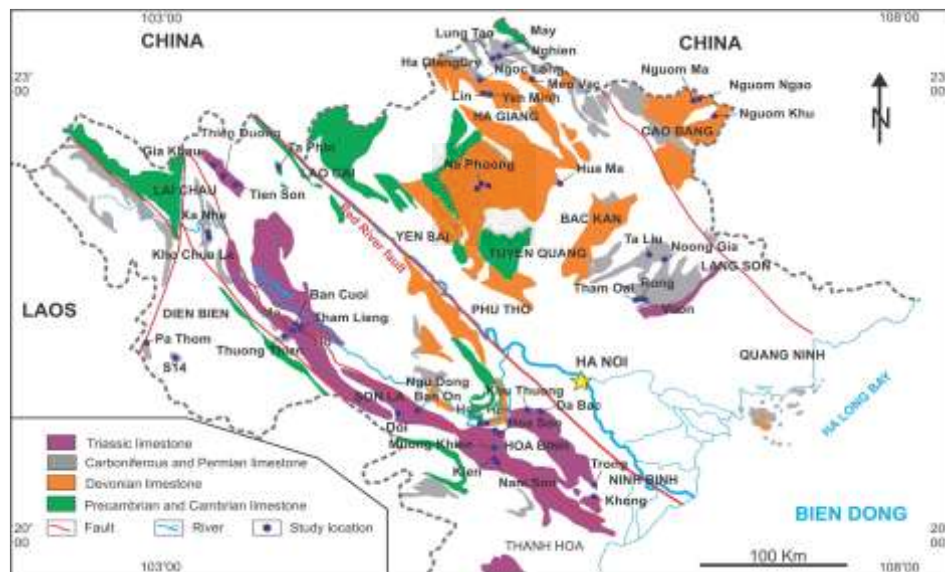


Figure 1. Distribution map of carbonate formations in Northern Vietnam and locations of surveyed caves in this study (The Department of Geology and Minerals of Vietnam, 2005; Phan et al., 1991).
Upper-case names indicate provinces

Table 1. List of surveyed caves in Northern Vietnam

No	Cave Names	Location (Lat.; Long.)	Humidity (maximum)	Survey time	Stalagmite characteristics	Sample collection
1	Vuon	Lang Son (21°35'; 106°14')	99%	2008	Not many stalagmites	2 broken stalagmites
2	Rong	Lang Son (21°35'; 106° 12')	99%	2008, 2009	Not many stalagmites	2 broken stalagmites
3	Tham Oai	Lang Son (21°35'; 106°11')	99%	2008	Not many stalagmites	1 broken stalagmite
4	Noong Gia	Lang Son (21°51'; 106°22')	99%	2008	Not many stalagmites	2 broken stalagmites
5	Ta Liu	Lang Son (21°52'; 106°16')	99%	2008	Not many stalagmites	1 broken stalagmite
6	Ha Giang Dry	Ha Giang (23°03'; 105°05')	99%	2010	Not many stalagmites	1 broken stalagmite
7	Ngoc Long	Ha Giang (23°03'; 105°04')	99%	2010, 2012	Not many stalagmites	5 broken stalagmites
8	Lin	Ha Giang (22°57'; 105°58')	99%	2010	Not many stalagmites	6 broken stalagmites
9	Yen Minh	Ha Giang (22°59'; 105°58')	99%	2010	Not many stalagmites	2 broken stalagmites
10	Nghien	Ha Giang (23°08'; 105°13')	99%	2010	Not many stalagmites	3 broken stalagmites
11	Lung Tao	Ha Giang (23°09'; 105°14')	99%	2010	Not many stalagmites	3 broken stalagmites
12	May	Ha Giang (23°14'; 105°19')	99%	2010	Not many stalagmites	4 broken stalagmites
13	Meo Vac	Ha Giang (23°03'; 105°20')	99%	2010	Not many stalagmites	1 broken stalagmite
14	S14	Son La (21°18'; 103°15')	99%	2004, 2005, 2006	Many stalagmites	10 broken stalagmites
15	Thuong Thien	Son La (21°20'; 103°56')	99%	2005, 2006, 2023	Many stalagmites	10 broken stalagmites
16	Doi	Son La (21°20'; 103°57')	99%	2023	Not many stalagmites	4 broken stalagmites
17	Ma	Son La (21°20'; 103°58')	99%	2023	Not many stalagmites	2 broken stalagmites
18	Ho	Son La (21°20'; 103°58')	99%	2023	Not many stalagmites	2 broken stalagmites
19	Ban Cuoi	Son La (21°21'; 103°58')	99%	2023	Not many stalagmites	4 broken stalagmites
20	Tham Lieng	Son La (21°21'; 103°58')	99%	2023	Not many stalagmites	4 broken stalagmites
21	Ngu Dong Ban On	Son La (20°52'; 104°38')	85%	2018	Not many stalagmites	
22	Doi	Son La (20°52'; 104°37')	85%	2018	No stalagmites	
23	Khong	Ninh Binh (20°22'; 105°03')	85%	2017	Not many stalagmites	1 broken stalagmite

No	Cave Names	Location (Lat.; Long.)	Humidity (maximum)	Survey time	Stalagmite characteristics	Sample collection
24	Trong	Ninh Binh (20°22'; 105°54')	Open system	2017	No stalagmites	
25	Thien Duong	Lai Chau City (22°18'; 103°26')	99.9%	2018	Diversity of stalagmites	6 broken stalagmites
26	Thien Mon	Lai Chau City (22°18'; 103°26')	99.9%	2018	Diversity of stalagmites	6 broken stalagmites
27	Tien Son	Lai Chau (22°45'; 105°10')	99.9%	2015, 2016, 2018	Diversity of stalagmites	7 broken stalagmites
28	Gia Khau	Lai Chau City (22°46'; 103°19')	99.9%	2024	Not many stalagmites	3 broken stalagmites
29	Chin Chu Chai	Lai Chau (22°21'; 103°37')	99.9%	2024	Not many stalagmites	
30	Ta Phin	Lao Cai (22°24'; 103°50')	99.9%	2024	Not many stalagmites	
31	Thac Bo	Hoa Binh (20°44'; 105°07')	90%	2018	Not many stalagmites	
32	Khu Thuong	Hoa Binh (20°41'; 105°16')	85%	2018	Not many stalagmites	
33	Da Bac	Hoa Binh (20°49'; 105°36')	85%	2018	Not many stalagmites	
34	Hoa Son	Hoa Binh (20°43'; 105°19')	99.9%	2018–2024	Many stalagmites were broken	20 broken stalagmites
35	Khong Day	Hoa Binh (20°43'; 105°19')	99.9%	2018	Not many stalagmites	
36	Dong Hoa	Hoa Binh (20°44'; 105°07')	99.9%	2018	Not many stalagmites	
37	Nam Son	Hoa Binh (20°32'; 105°11')	99.9%	2018–2024	Many stalagmites; Some were broken	6 broken stalagmites
38	Muong Khien	Hoa Binh (20°37'; 105°16')	99.9%	2018	Not many stalagmites	2 broken stalagmites
39	Kien	Hoa Binh (20°32'; 105°10')	99.9%	2024	Not many stalagmites	3 broken stalagmites
40	Pa Thom	Dien Bien (21°16'; 102°51')	99.9%	2018	Not many stalagmites	
41	Kho Chua La	Dien Bien (21°52'; 103°24')	99.9%	2018	Not many stalagmites	
42	Xa Nhe	Dien Bien (21°52'; 103°25')	99.9%	2018	Not many stalagmites	
43	Nguom Khu	Cao Bang (22°47'; 106°46')	90%	2021	Not many stalagmites	
44	Nguom Ngao	Cao Bang (22°50'; 106°42')	99.9%	2021	Not many stalagmites	
45	Nguom Ma	Cao Bang (22°50'; 106°42')	95%	2021	Not many stalagmites	
46	Na Phoong	Bac Kan (22°18'; 105°31')	85%	2023	Not many stalagmites	
47	Pac Chai	Bac Kan (22°18'; 105°30')	85%	2023	Not many stalagmites	
48	Ban Piac	Bac Kan (22°18'; 105°30')	85%	2023	Not many stalagmites	
49	Dong Troi	Bac Kan (22°18'; 105°30')	85%	2023	Not many stalagmites	
50	Tham Thinh	Bac Kan (22°18'; 105°29')	90%	2023	Not many stalagmites	
51	Hua Ma	Bac Kan (22°21'; 105°40')	99.9%	2023	Many stalagmites; Some were broken	4 broken stalagmites

2.3. Climate conditions

The general characteristics of the climate in Northern Vietnam are a tropical monsoon climate, low radiation balance, limited sunshine, low temperatures, and a cold winter (Nguyen & Nguyen, 2004). According to CRU TS4.08 data (University of East Anglia Climatic Research Unit et al., 2024), Northern Vietnam's average annual temperature is 22.2°C, with a precipitation total of 1593 mm. The region exhibits a tropical monsoon climate, characterized by a pronounced wet season from May to October (Fig. 2). Annual rainfall ranges from 120 to

160 days, with 80–90% of precipitation concentrated in these months. Dry conditions prevail from November to March, with monthly rainfall averaging 24–49 mm and rarely exceeding 100 mm. During the wet season, precipitation ranges from 100 to 306 mm per month, peaking in July, with a mean temperature of 27.6°C; extreme daily maxima occur in June (41°C on June 4 and 5, 2021). The Köppen-Geiger classification designates lowland areas as 'Cwa' (humid subtropical with dry winter) and highlands as 'Cwb' (subtropical highland with dry winter) (Beck et al., 2018).

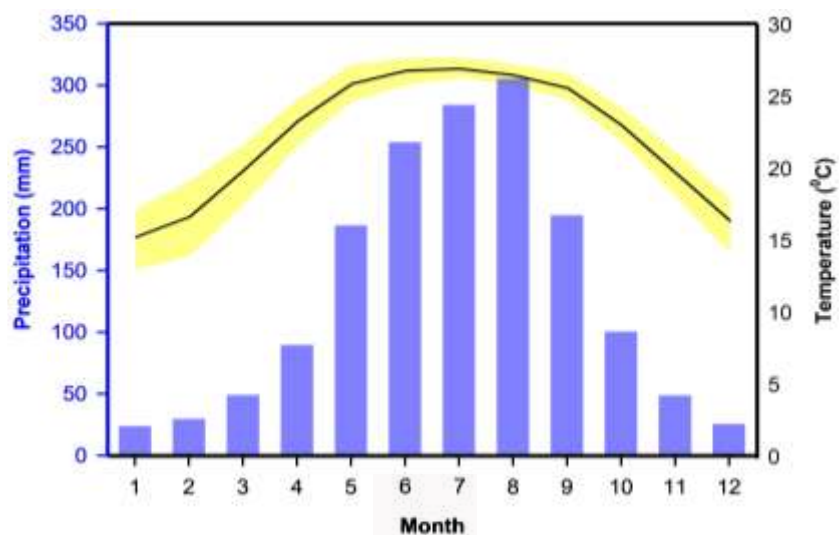


Figure 2. Monthly temperature and precipitation averages (1901–2023) for northern Vietnam (19–24°N, 102–109°E), from CRU TS4.08 (University of East Anglia Climatic Research Unit et al., 2024). Data were generated in the KNMI Climate Explorer (van Oldenborgh, 2020)

Northern Vietnam is divided into three distinct climatic regions: the Northwest, the Northeast, and the Red River Delta. Among the surveyed provinces, Son La, Dien Bien, and Lai Chau belong to the Northwest region; Lao Cai, Ha Giang, Cao Bang, and Bac Kan belong to the Northeast region; and Hoa Binh and Ninh Binh belong to the Red River Delta region. These three climatic

regions share the general characteristics of Northern Vietnam's climate, characterized by cold winters and hot summers. The climatic parameters show slight variation between the Northwest and Northeast zones. The Red River Delta region experiences higher temperatures and a narrower temperature range compared to the other areas (Table 2).

Table 2. Comparison of the three climatic zones in Northern Vietnam (summarized from Nguyen & Nguyen, 2004)

Climate zone	T _{tb}	T _{Mmax} / T _{Mmin}	T _{max} / T _{min}	R	RH	E	Other characteristics
Northwest zone	18–22	26–27/13–16	38–40/-2–2	1200–2000	82–85	800–1000	Relatively abundant sunshine in winter, occasional frost in some years, and slight drizzle; Hot in summer with frequent dry and hot westerly winds, not directly affected by storms and tropical depressions
Northeast zone	18–23	26–28/12–16	38–41/-2–2	1400–2000	82–85	600–1000	Little sunshine in winter, occasional frost in some years, and frequent drizzle. Hot summer with minimal dry and hot westerly winds, directly affected by numerous tropical cyclones, especially in the Northeast, and experiences heavy rainfall.
Red River delta zone	23–24	28–29/15–16,5	38–41/2–5	1400–1800	82–85	700–800	

Notes: T_{tb}. Annual average temperature (°C); T_{Mmax}/T_{Mmin}. Temperature of the hottest month/Temperature of the coldest month (°C); T_{max}/T_{min}. Absolute highest/lowest temperature (°C); R. Rainfall (mm/year); RH. Relative humidity (%); E. Evaporation (mm/year)

2. Materials and methods

We systematically surveyed 51 caves across Northern Vietnam from 2017 to 2024, collecting 127 broken stalagmites (Table 1) to evaluate their suitability as paleo-monsoon archives. In paleoclimate studies, a high-quality stalagmite resembles a candle or a long, circular cylinder. The diameter remains constant from the bottom to the top. These form in long, narrow caves with closed entrances, where humidity exceeds 95%. It also forms in narrow niches at the ends of caves (Hendy, 1971). We used a 77535 AZ Portable CO₂ Analyzer to measure temperature and humidity at the entrance and in various parts of all caves (Fig. 3a). During our survey, we observed and recorded the potential for collecting stalagmites, and collected broken potential stalagmites (Fig. 3). In the caves where the maximum

humidity reached 99.9%, we collected all broken promising stalagmites. For caves with humidity below 95%, we collected at least one stalagmite, if available, to assess their potential for use in paleoclimate studies. We labelled the samples using the cave name abbreviation and numbered them in order of collection. For example, 20 samples were collected from the Hoa Son cave and labelled HS1–HS20.

After collection, samples were cut in half, washed with distilled water, and polished for photography and description. Samples were then washed in an ultrasonic bath with distilled water to ensure no impurities were mixed into the stalagmites prior to subsampling for the Hendy Test. The Hendy test is a classic diagnostic tool used in speleothem paleoclimatology to check whether the oxygen isotope values ($\delta^{18}\text{O}$) in a speleothem reflect

equilibrium deposition rather than kinetic effects (such as evaporation or rapid degassing). Equilibrium deposition is a critical requirement for using speleothems as reliable $\delta^{18}\text{O}$ and $\delta^{13}\text{C}$ proxies (Hendy, 1971; Dorale et al., 1992). Powdered subsamples weighing 200 to 300 μg were collected from the polished surface of selected stalagmites using a handheld carbide dental drill. Subsamples were drilled on a class-100 clean bench in a class-10000 pretreatment room for measurements of C/O stable isotopes and U/Th dating. To prevent cross-contamination, the drill bit was thoroughly cleaned with 2 N HCl and alcohol before extracting each subsequent subsample. For the Hendy test, we selected two thick, clean layers and extracted

at least five subsamples per layer using a dental drill fitted with fine bits. Each drill hole had a diameter of less than 0.5 mm and a depth of approximately 2 mm. In accordance with these specifications, the subsamples intended for Hendy tests were analyzed using a Micromass IsoPrime mass spectrometer at the Department of Earth Sciences, National Taiwan Normal University. The measured results were then processed and calculated in Excel. All $\delta^{18}\text{O}$ values are expressed in parts per thousand (or per mil with symbol ‰) relative to the Vienna Pee Dee Belemnite (VPDB), with standardization performed using NBS-19. The reproducibility of the $\delta^{18}\text{O}$ measurements was $\pm 0.08\text{--}0.12\text{‰}$ at the 1-sigma level.



Figure 3. Measuring humidity and temperature (a) at the entrance and (b) 52 m from the entrance of Hua Ma cave. (c) A broken stalagmite collected in Hua Ma cave

U/Th dating of subsamples from top and bottom layers of selected stalagmites was performed using a Thermo Scientific NEPTUNE MC-ICP-MS (multi-collector inductively coupled plasma mass spectrometer) at the Department of Geosciences, National Taiwan University, following Shen et al. (2012). Each subsample, weighing 30–100 mg, was drilled along horizons using a handheld carbide dental burr,

following the methodology outlined in Dorale et al. (2007). Uranium (U) and thorium (Th) chemical separation and purification procedures were adapted from Edwards et al. (1987) and Shen et al. (2002). The decay constants used were $9.1705 \times 10^{-6} \text{ yr}^{-1}$ for ^{230}Th (Cheng et al., 2013), $2.8215 \cdot 10^{-6} \text{ yr}^{-1}$ for ^{234}U (Hu et al., 2025), and $1.55125 \times 10^{-6} \text{ yr}^{-1}$ for ^{238}U (Jaffey et al., 1971). Corrected ages relative to CE 1950 were

calculated using an assumed initial $^{230}\text{Th}/^{232}\text{Th}$ atomic ratio of $4 \pm 2 \times 10^{-6}$. Uncertainties from all sources were propagated through the U-Th age calculations and reported at the 2σ level, unless otherwise specified. The detailed offline data reduction and age calculations followed the method described by Shen et al. (2002).

3. Results

3.1. Humidity and availability of stalagmites

Previous studies have shown that humidity conditions influence the ability of speleothems to form under isotopic equilibrium (Fairchild et al., 2006; McDermott et al., 2004; Lachniet, 2009). High relative humidity (typically $\geq 95\%$) within caves minimizes evaporation, allowing drip water to precipitate calcite or aragonite under near-equilibrium conditions, as indicated by stable oxygen and carbon isotopes (McDermott, 2004). In contrast, lower humidity can enhance evaporation, leading to isotopic enrichment (especially in $\delta^{18}\text{O}$), which distorts paleoclimate signals (Markowska et al., 2016). Therefore, maintaining saturated cave air is essential for reliable speleothem-based paleoclimate reconstructions.

Of the 51 caves surveyed, 37 exhibited relative humidity levels of 99,9%. This includes all 5 caves in Lang Son province, all 8 caves in Ha Giang province, 7 of 9 caves in Son La province, all 6 caves in Lai Chau province, the cave in Lao Cai province, 1 of 6 caves in Bac Kan province, 1 of 3 caves in Cao Bang province, all 3 caves in Dien Bien province, and 5 of the 8 caves in Hoa Binh (Table 1).

Among the 37 caves with high humidity, only a few featured a rich diversity of

speleothem formations, including the Hoa Son and Nam Son caves (Hoa Binh Province), S14 and Thuong Thien (Son La Province), Thien Duong, Thien Mon, and Tien Son (Lai Chau), as well as Hua Ma (Bac Kan province) (Fig. 5c, Fig. 5e, Fig. 5f). Field surveys at these caves revealed that stalagmites have been extensively broken in Hoa Son, Thien Duong, and Thien Mon caves, likely due to poorly managed tourism activities (Figs. 5a, b, d). Nam Son Cave is magnificent and features a rich diversity of speleothem formations, especially stalagmites (Figs. 5e, f). Because it is strictly managed and kept locked when not open to visitors, the number of broken stalagmites is minimal. Hua Ma Cave is also developed for tourism, but the number of damaged speleothems remains relatively low (Fig. 5c). Tien Son Cave has abundant stalagmite formations; however, due to inadequate management, the cave was flooded during a storm in 2021, covering many speleothems in a thick layer of mud.

Although the Trang An Complex in Ninh Binh Province is a large limestone area, its cave system is primarily an open one, with a river flowing through the caves. Therefore, we selected only two promising caves (Khong Cave and Trong Cave) in this area in 2017. The Trong cave showed an open system with two huge entrances, and no stalagmites were found. The Khong cave has the characteristics of a closed cave system with one entrance and a very dark, narrow, and low path (Fig. 4a, b); however, the humidity of the cave is not saturated (Table 1). The number of stalagmites found in this cave is also limited. Among the caves with $<95\%$ maximum humidity, we selected Khong Cave to collect a stalagmite sample for testing the suitability of stalagmites in paleoclimate research (Fig. 4d).

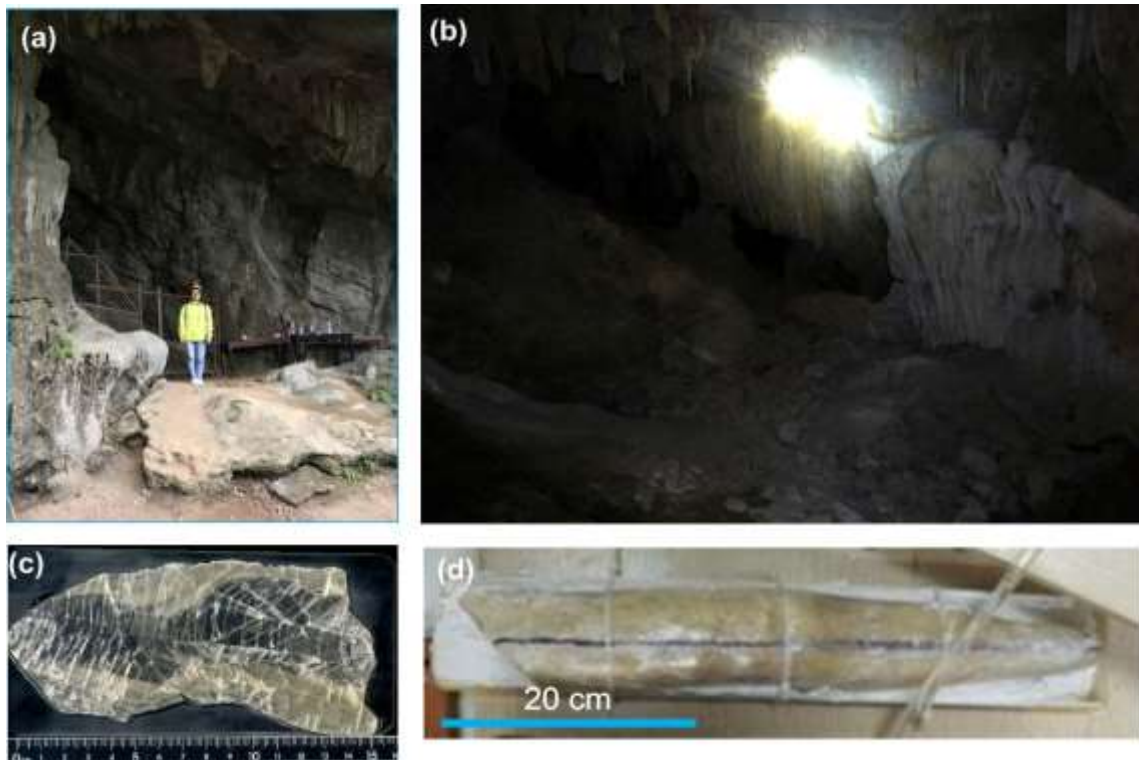


Figure 4. The Khong cave: (a) The entrance, (b) 62 m from the entrance, (c) thin section (slab), and (d) broken stalagmites

3.2. Classification of stalagmites to select samples for paleoclimate study

To select suitable samples for paleoclimate analysis, we classified all stalagmites collected from the 51 surveyed caves into five groups based on purity, porosity, and growth-layer features (Table 3). Some stalagmites are selected for display in Fig. 6. The reasons for this classification are as follows:

- Speleothems with high porosity and a spongy internal structure are often associated with precipitation under isotopic disequilibrium conditions (Mickler et al., 2006; Frisia, 2015; Dreybrodt & Scholz, 2011). This texture can result from rapid CO_2 degassing, evaporation, or high drip rates that hinder equilibrium fractionation between water and calcite (Mühlinghaus et al., 2009). Such fabrics typically exhibit kinetic effects that cause $\delta^{18}\text{O}$ and $\delta^{13}\text{C}$ values to deviate

from their expected equilibrium values. Therefore, petrographic analysis of speleothem structure can serve as a diagnostic tool for assessing the reliability of isotopic data.

- Contamination in speleothems, such as detrital particles, mud layers, and inorganic inclusions, can significantly affect the accuracy of U/Th dating. These impurities introduce excess ^{232}Th , which is not part of the radioactive decay chain used in age calculation, leading to artificially old or reversed ages (Labonne et al., 2002; Wortham et al., 2022). In some cases, the presence of dirty layers requires extensive correction models or renders certain sections unsuitable for precise dating (Sánchez-Moreno et al., 2022). Consequently, only clean, well-preserved calcite/aragonite layers are considered reliable for establishing high-resolution paleoclimate chronologies.

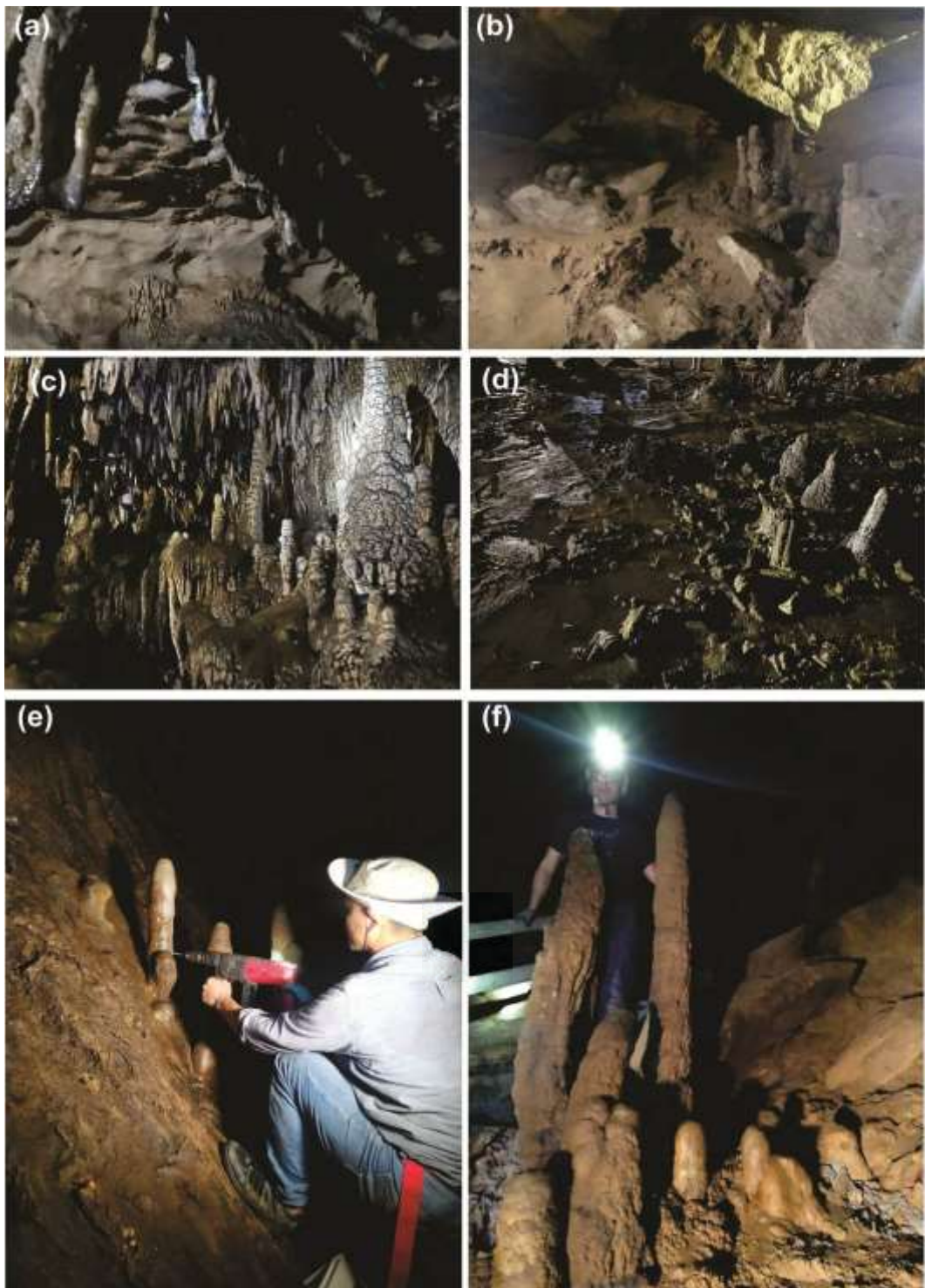


Figure 5. Examples of stalagmite specimens from some selected caves

Table 3. Classification of stalagmites collected in Northern Vietnam

Group	Stalagmites' ID	Characteristics
1	CB03, GK01, GK02, HS3, HS15, HS16, HS13, HS19, HK02, NS3, TT-03, TT-05, TT23-01, TT23-02, TT23-03	Well-defined crystalline layers with high purity
2	HS5, HS7, HS12, HS18, HM01, LS1.1, NS4, NS6, S16, TD01, TD02, TD04, TL01, TL02, TL03, TM01, TT23-04, TT23-14, TT23-15, TT23-17	Well-defined crystalline layers with high purity and no porosity, and/or some layers are contaminated, porous, or irregular, discontinuous growth layers
3	HK03, HH01, HH02, HS2, HS4, HS9a, HM02, HMA01, HS9b, HS10, HS11, HS15, HS20, Lin01, Lin02, LS1.2, LS2.1, LS2.2, MC1, NL-02, NS2, S14-9, TK04, TM03, TM05, TD05, TL04, TL05, TL06, TS02, TT23-06, TT23-13, TT23-16, YM02-1, YM02-2	Some layers are contaminated and/or porous, irregular, and discontinuous growth layers.
4	NS5, CB01, CB02, CB03, LS4.1, LS4.2, LS5.1, Lin03, May01-1, May02, May03, TK01, TK02, TK03, TT23-05, TT23-07,	Crystalline layers with low purity and high porosity
5	CB04, CB05, CB06, NS1, HS1, HS8, HS14, HS17, HS20, HK01, HK03, MC2, GK03, TM02, TM04, TD03, LS3.1, MV01, NG-03, TL07, TT23-08, TT23-09,	Visibly porous

- Irregular and discontinuous growth layers in stalagmites can significantly limit their usefulness for paleoclimate reconstruction. Such growth interruptions often result from changes in hydrological conditions, cave ventilation, or surface vegetation, and may introduce large chronological gaps or age inversions in U/Th dating (Fairchild & Baker, 2012; Scholz & Hoffmann, 2011). These discontinuities complicate the development of continuous time series and reduce confidence in interpreting climate signals. Therefore, only stalagmites with continuous, clearly laminated growth and minimal hiatuses are preferred for high-resolution paleoclimate studies.

3.3. Selecting stalagmites for U/Th dating and the Hendy Test

Based on purity, porosity, and stable growth, the stalagmites with potential for use in paleoclimate research are ranked from highest to lowest, with group 1 as the highest and group 5 as the lowest. We prioritized samples from groups 1 and 2 to select for U/Th dating and the Hendy Test. Some samples from other groups that show potential, for example, certain parts of the stalagmites that exhibit high purity, low porosity, and stable growth, were also selected for U/Th dating. Based on this

principle, 5 stalagmites from group 1 including TT-03, TT-05, NS3, HS16, and HS3, 1 stalagmite from group 2 (HS7), 1 stalagmite from group 4 (NS5), 1 stalagmite from group 3 (HS9b), and 1 stalagmite from group 5 (HS17) was selected for U/Th dating; TT-03, TT-05, NS3, HS3 and HS16 from the group 1 and HS7 from the group 2 were selected for the Hendy test.

3.4. U/Th dating

Samples from the pure layers at the uppermost (Top) and lowermost parts (Bottom) of each stalagmite were subsampled for U/Th dating. In total, 18 subsamples were collected for U/Th dating (Table 6). ^{238}U concentrations of the samples from group 1 ranged from 2.112 to 61.823 ppm, and ^{232}Th concentrations varied from 36.9 to 2292.0 ppt, with dating errors typically below 0.5% (Table 6).

^{238}U concentrations of the sample from groups 2, 3, 4, and 5 ranged from 6.951 to 11.652 ppm, and ^{232}Th concentrations varied from 44.3 to 2561 ppt, with dating errors typically below 0.5% (Table 6). ^{238}U concentrations of the sample from group 4 are 0.358 and 7.306 ppm, and ^{232}Th concentrations are 354.3 to 1153.1 ppt, with dating errors typically below 0.5%.

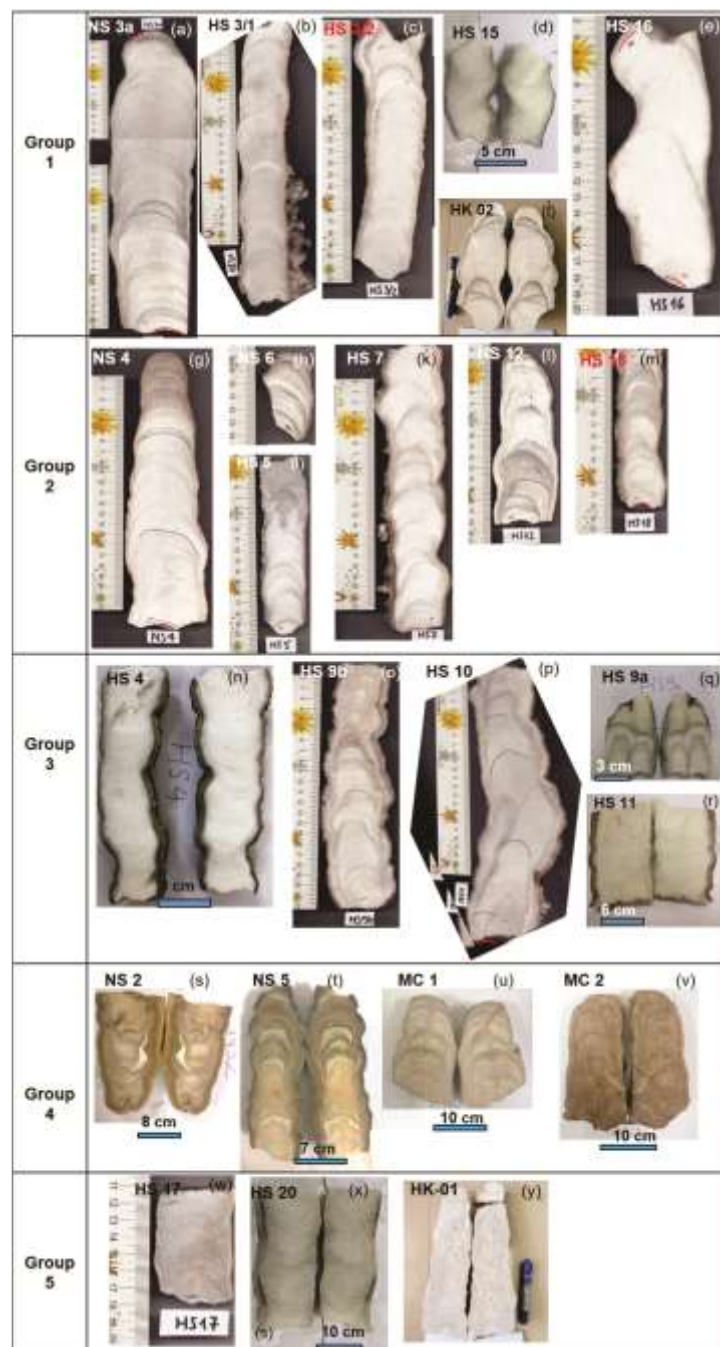


Figure 6. Classification of stalagmites in some selected caves into 5 groups

3.5. Hendy test results

A total of 56 subsamples were collected for stable isotope analysis using the Hendy Test method (Table 4, Fig. 7). Across all

layers, $\delta^{18}\text{O}$ and $\delta^{13}\text{C}$ values show small 1 sigma variations ($<0.2\text{‰}$) and weak correlations ($R^2 < 0.3$), consistent with deposition under near isotopic equilibrium (Table 5, Fig. 7).

Table 4. The $\delta^{18}\text{O}$ and $\delta^{13}\text{C}$ results of stalagmites NS3, HS3, HS7 and HS16

Sample ID	Layer	Sub-sample	$\delta^{18}\text{O}$ (‰, VPDB)	$\delta^{13}\text{C}$ (‰, VPDB)	Sample ID	Layer	Sub-sample	$\delta^{18}\text{O}$ (‰, VPDB)	$\delta^{13}\text{C}$ (‰, VPDB)
NS3	1	1	-7.92	-3.97	HS3	1	1	-7.77	-3.77
		2	-8.03	-4.02			2	-7.82	-3.82
		3	-8.11	-4.01			3	-7.79	-3.79
		4	-7.95	-3.99			4	-7.81	-3.81
		5	-8.07	-4.03			5	-7.78	-3.78
		6	-8.00	-3.98			6	-7.80	-3.80
		7	-7.99	-4.01			7	-7.76	-3.76
	2	1	-8.20	-4.13		2	1	-7.87	-3.87
		2	-8.05	-4.09			2	-7.92	-3.92
		3	-8.15	-4.11			3	-7.89	-3.89
		4	-8.09	-4.07			4	-7.91	-3.91
		5	-8.18	-4.12			5	-7.88	-3.88
		6	-8.10	-4.10			6	-7.90	-3.90
		7	-8.13	-4.08			7	-7.86	-3.86
HS7	1	1	-7.40	-2.00	HS16	1	1	-8.17	-4.17
		2	-7.52	-2.80			2	-8.22	-4.22
		3	-7.68	-3.10			3	-8.19	-4.19
		4	-7.45	-2.20			4	-8.21	-4.21
		5	-7.60	-2.90			5	-8.18	-4.18
		6	-7.49	-2.30			6	-8.20	-4.20
		7	-7.56	-2.70			7	-8.16	-4.16
	2	1	-7.50	-2.10		2	1	-8.27	-4.27
		2	-7.62	-2.90			2	-8.32	-4.32
		3	-7.78	-3.20			3	-8.29	-4.29
		4	-7.55	-2.30			4	-8.31	-4.31
		5	-7.70	-3.00			5	-8.28	-4.28
		6	-7.59	-2.40			6	-8.30	-4.30
		7	-7.66	-2.80			7	-8.26	-4.26

Table 5. Hendy test results of stalagmites NS3, HS3, HS7, HS16

Stalagmite	Layer	$\delta^{13}\text{C}$ range (‰)	$\delta^{18}\text{O}$ range (‰)	$1\sigma \delta^{13}\text{C}$ (‰)	$1\sigma \delta^{18}\text{O}$ (‰)	$R^2 (\delta^{13}\text{C} \text{ vs } \delta^{18}\text{O})$
NS3	1	-4.64 to -4.94	-6.37 to -6.76	± 0.08	± 0.14	0.23
	2	-5.01 to -5.12	-7.72 to -8.16	± 0.04	± 0.16	0.24
HS3	1	-3.67 to -4.07	-6.13 to -6.35	± 0.13	± 0.07	0.03
	2	-3.89 to -4.40	-6.11 to -6.36	± 0.16	± 0.09	0.08
HS7	1	-2.71 to -4.81	-7.07 to -7.32	± 0.13	± 0.07	0.24
	2	-3.13 to -3.83	-7.37 to -7.60	± 0.16	± 0.09	0.74
HS16	1	-4.27 to -5.51	-7.16 to -7.63	± 0.13	± 0.07	0.02
	2	-4.61 to -5.61	-7.83 to -7.92	± 0.16	± 0.09	0.03
TT-3	1	-6.11 to -6.57	-7.31 to -7.47	± 0.14	± 0.05	0.15
	2	-5.18 to -5.45	-7.00 to -7.27	± 0.08	± 0.14	0.13
	3	-5.61 to -6.06	-7.74 to -7.93	± 0.15	± 0.07	0.27
TT-5	1	-5.08 to -5.79	-6.38 to -6.85	± 0.11	± 0.01	0.28
	2	-5.23 to -6.01	-7.43 to -7.90	± 0.23	± 0.15	0.11
	3	-5.13 to -5.37	-7.55 to -8.05	± 0.07	± 0.15	0.33
	4	-5.70 to -6.24	-7.80 to -8.07	± 0.19	± 0.11	0.23

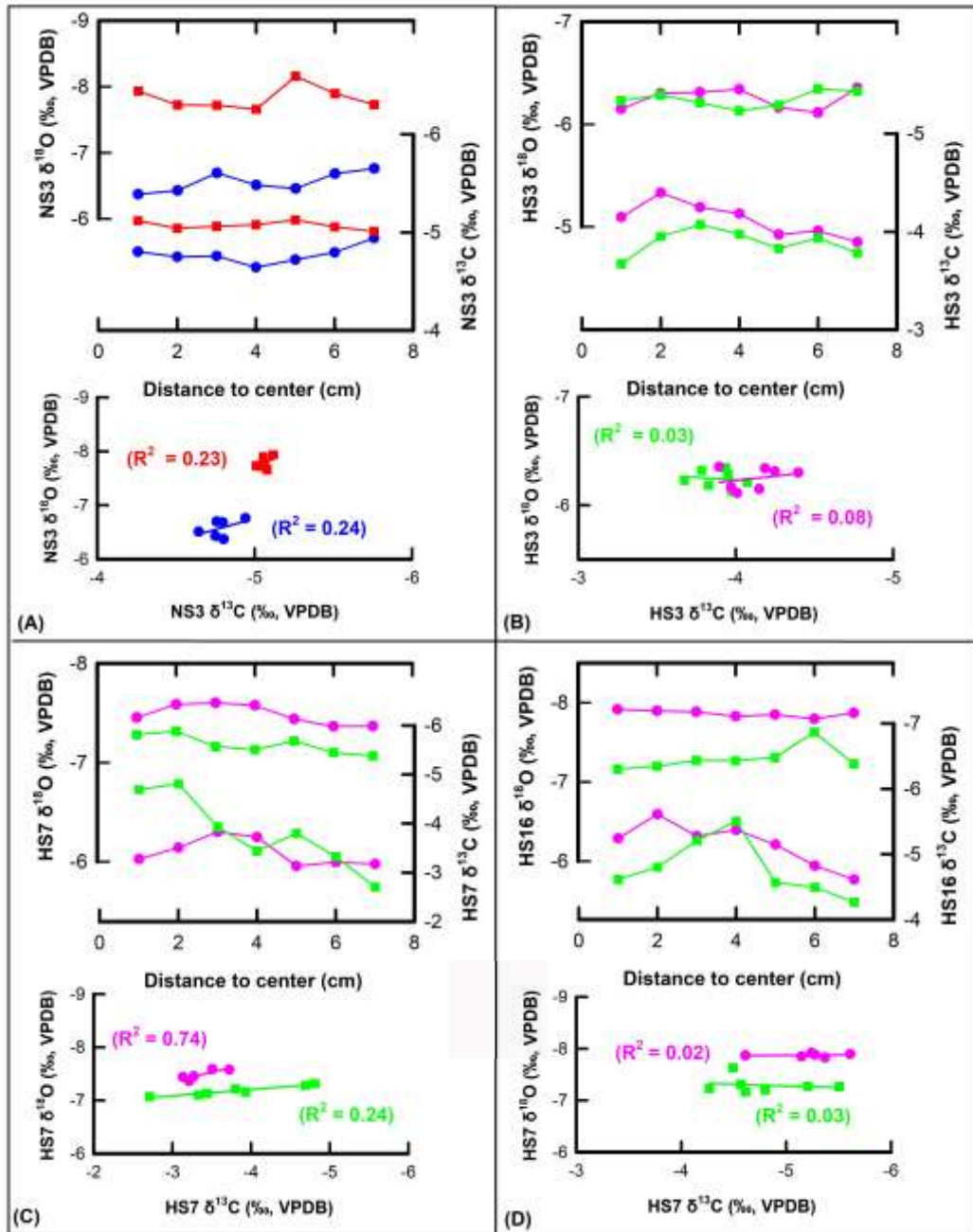


Figure 7. Visualizations of Hendy test results of stalagmites NS3 (A), HS3 (B), HS7 (C), HS16 (D)

The Hendy test, conducted on the two stalagmites, TT-3 and TT-5, shows stable $\delta^{18}\text{O}$ values throughout the growth layers, with no significant enrichment away from the growth axis. Furthermore, no systematic

correlation between $\delta^{18}\text{O}$ and $\delta^{13}\text{C}$ was observed with increasing distance from the axis, as evidenced by low correlation coefficients (Nguyen et al., 2020, 2022).

4. Potential for collecting high-quality samples from caves in the North of Vietnam for paleoclimate study

4.1. The potential area in the North of Vietnam

Our systematic survey of 51 caves in Northern Vietnam demonstrates that stalagmites from this region hold significant potential as archives for reconstructing paleomonsoon dynamics, a critical aspect of Southeast Asian paleoclimate research. Our field trip results indicate that among the surveyed provinces in northern Vietnam, Lai Chau, Son La, and Hoa Binh have the greatest potential to yield high-quality stalagmites for paleoclimate studies. All five caves in Lai Chau province had maximum humidity levels of 99.9%. However, only the Tien Son and Thien Duong caves show potential for collecting stalagmites for paleoclimate reconstructions, due to the limited growth of stalagmites in the Gia Khau and Chin Chu Chai caves. Stalagmites also grow well in Thien Mon Cave; however, it has two entrances and humidity is unstable. So the stalagmites in Thien Mon cave may not be suitable for paleoclimate studies.

Field trips to 9 caves in Son La province provided insights into their suitability for stalagmite-based paleoclimate studies, during which 36 stalagmites were collected. Of these, two caves recorded maximum humidity levels below 95%, indicating less favorable conditions for equilibrium deposition, while the remaining seven caves exhibited maximum humidity levels above 95% (Table 1). Among the high-humidity caves, including Thuong Thien, only two stood out for their numerous stalagmites, suggesting greater potential for paleoclimate research owing to their abundance and physical condition.

4.2. Criteria for Selecting Suitable Speleothems for U/Th Analysis and Paleoclimate Studies

Published studies have shown that cave humidity, speleothem purity, porosity, and the stability of the growth axis significantly influence the isotopic equilibrium conditions during speleothem formation and the accuracy of U/Th dating. Consequently, these factors affect the reliability of speleothems for paleoclimate reconstruction. In our study, we classified the speleothem samples based on the humidity of the sampling site, their purity, porosity, and the stability of their growth axis to select appropriate specimens for analysis. Following these criteria, we found that this method of sample selection was entirely suitable. Speleothems collected from caves with low humidity exhibited post-depositional recrystallization. Moreover, speleothems in group 1 exhibited better isotopic equilibrium than those in group 2.

Visibly porous speleothems are generally unsuitable for paleoclimate studies because they are vulnerable to post-depositional alteration, which compromises the integrity of geochemical proxies such as $\delta^{18}\text{O}$ and $\delta^{13}\text{C}$. Their porous structure allows for recrystallization and isotopic exchange, as water and air in the cave environment can infiltrate and alter the original chemical signals. This leads to unreliable reconstructions of past climate variables, such as temperature and precipitation.

Additionally, porous speleothems are less suitable for precise dating methods, such as uranium-thorium dating, which require dense, unaltered calcite to ensure accuracy. In contrast, dense, compact speleothems are preferred because they act as sealed time capsules, preserving stable-isotopic and trace-element records that are essential for accurate paleoclimate reconstructions.

Our thin-section analysis of a stalagmite slab collected from Khong cave, Ninh Binh

province, shows that the original aragonite was transformed into calcite (Fig. 4c), leading to the loss of paleoclimatic information recorded in stalagmites. The cave's unsaturated humidity may have caused this transformation. These results indicate that identifying suitable stalagmites for paleoclimate studies in the Trang An complex, Ninh Binh province, is challenging, and that cave humidity correlates with stalagmite quality. The result aligns with McDermott's (2004) conclusion regarding the influence of humidity conditions on the ability of speleothems to form under isotopic equilibrium. Consequently, caves that are suitable for collecting high-quality stalagmites for paleoclimate studies should have humidity levels exceeding 95%.

The purity of the sample can affect the dating error. The analysis of selected samples from groups 1 and 2 revealed that the minimum uranium content required for accurate ^{230}Th measurement through multi-collector inductively coupled plasma mass spectrometry (MC-ICP-MS) is approximately 50–100 ppb; ideally, speleothems with higher uranium concentration are always more favorable for U-Th dating (Cheng et al., 2013; Chiang et al., 2019; Shen et al., 2012). The results indicate that high-potential samples were found in caves in Hoa Binh province. Samples such as NS3 and HS3, which are enriched in karstic geology (Sterling, 2006), meet this threshold, whereas their low-uranium counterparts exhibit elevated age errors (Scholz & Hoffmann, 2011).

The purity of the sample is not only restricted to uranium contents but also to thorium. Maintaining low detrital thorium contamination is critical, with a $^{230}\text{Th}/^{232}\text{Th}$ activity ratio greater than 20 (ideally above 100) to minimize correction for initial ^{230}Th (Henderson, 2006). Initial U/Th data from nine stalagmites (Table 6) suggest a potential investigation of paleoclimate using stable isotopes as proxies. Among the sub-samples

collected for U/Th analysis, the NS5-bottom sample had the lowest purity, and the HS9b-bottom had the highest porosity. The U content in NS5-bottom was the lowest, but still within the allowable limit. In contrast, the U content in HS9b-bottom is high, but the dating error is relatively high, at 0.7%. This multi-site approach contrasts with Nguyen et al.'s (2020) single-cave focus, providing a regional baseline for Southeast Asian speleothem studies (Nguyen et al., 2022; Wolf et al., 2023). The U/Th dating results indicate late Quaternary spans for the selected stalagmites (Table 6), with growth rates exceeding 0.09 mm/year, suggesting potential for high-resolution records (Shen et al., 2012; Cheng et al., 2013).

Among the six selected stalagmites, the $\delta^{18}\text{O}$ values in the five stalagmites from group 1 remain relatively stable throughout their growth layers. Furthermore, the weak correlation between $\delta^{18}\text{O}$ and $\delta^{13}\text{C}$ ($R^2 < 0.25$) indicates that the isotopic variations are largely independent, implying precipitation under near-equilibrium conditions where kinetic fractionation was minimal (see Fig. 7A, B, D). Such weak $\delta^{18}\text{O}$ – $\delta^{13}\text{C}$ coupling is characteristic of isotopic equilibrium, as kinetic processes (e.g., rapid CO_2 degassing or evaporation) typically drive both isotopic ratios to vary in the same direction, producing a strong positive correlation. While the correlation value of the $\delta^{18}\text{O}$ and $\delta^{13}\text{C}$ of subsamples collected from layer 2 of HS7, the stalagmite collected from group 2, is 0.74, which is higher than 0.4, indicating that this stalagmite formed under non-equilibrium conditions (see Fig. 7C).

Continuous growth (exceeding 0.09 mm/year) has been shown to minimize depositional hiatuses, as sustained drip flux and constant supersaturation promote uninterrupted calcite precipitation (Ford & Williams, 2010). The U/Th dating results for NS3, HS3, HS7, and HS16 indicate growth rates above this threshold, with dating uncertainties of less than 0.5% (Table 6).

Among them, HS7 differs from the group 1 stalagmites primarily in the stability of its growth axis. The irregular lamination pattern of HS7 likely reflects short-term

disequilibrium conditions during deposition, whereas HS3 and HS16 collected from the same cave display geochemical characteristics consistent with isotopic equilibrium.

Table 6. Uranium and thorium isotopic compositions and ages by MC-ICPMS, Thermo Electron Neptune, at National Taiwan University

Sample name	^{238}U		^{232}Th	$\delta^{234}\text{U}$	$[^{230}\text{Th}/^{238}\text{U}]$	$^{230}\text{Th}/^{232}\text{Th}$	Age (ka)	Age (ka BP)	$\delta^{234}\text{U}_{\text{initial}}$
	10^{-9} g/g	10^{-12} g/g	measured	activity	atomic ($\times 10^{-6}$)	uncorrected	corrected ^{c,d}	corrected	
HS3-Top	6714	± 17	36.9	± 10	-15.8 ± 2.7	0.3912 ± 0.0011	1174804 ± 309450	55.33 ± 0.29	55.26 ± 0.29
HS3-Bottom	10945	± 32	222.2	± 9.0	10.7 ± 3.1	0.4270 ± 0.0014	346804 ± 13978	59.80 ± 0.37	59.73 ± 0.37
HS7-Top	11652	± 56	340.2	± 10	9.3 ± 5.1	0.3346 ± 0.0020	188957 ± 5392	43.88 ± 0.43	43.82 ± 0.43
HS7-Bottom	9102	± 30	548.1	± 8.6	13.7 ± 3.2	0.3470 ± 0.0015	95005 ± 1514	45.64 ± 0.31	45.57 ± 0.31
HS9b-Top	7299	± 32	2561.8	± 9.4	122.0 ± 2.6	0.76472 ± 0.00247	35923 ± 146	120.98 ± 0.90	120.90 ± 0.90
HS9b-Bottom	6951	± 32	397.6	± 8.1	122.6 ± 2.7	0.79259 ± 0.00197	228436 ± 4653	129.99 ± 0.88	128.92 ± 0.88
HS16-Top	9939	± 31	51.5	± 10	14.1 ± 3.1	0.3410 ± 0.0014	1084905 ± 201521	44.64 ± 0.29	44.57 ± 0.29
HS16-Bottom	10689	± 32	351.4	± 9.0	12.2 ± 2.9	0.3470 ± 0.0012	174068 ± 4491	45.74 ± 0.27	45.67 ± 0.27
HS17-Top	9557	± 69	187.6	± 8.3	41.7 ± 3.1	0.16775 ± 0.00059	140935 ± 6253	19.13 ± 0.10	19.06 ± 0.10
HS17-Bottom	9924	± 63	44.3	± 6.7	41.9 ± 3.2	0.18936 ± 0.00065	699826 ± 105730	21.84 ± 0.11	21.78 ± 0.11
NS3-Top	6709	± 16	813.9	± 6.9	54.5 ± 2.8	0.29692 ± 0.00087	40357 ± 348	35.95 ± 0.17	35.88 ± 0.17
NS3-Bottom	3290	± 6	326.8	± 9.1	41.3 ± 2.4	0.32176 ± 0.00074	53407 ± 1485	40.20 ± 0.16	40.13 ± 0.16
NS5-Top	7306	± 21	1153.1	± 7.7	151.0 ± 3.0	0.42134 ± 0.00138	44016 ± 300	49.16 ± 0.26	49.08 ± 0.26
NS5-Bottom	358	± 6	354.3	± 8.4	282.7 ± 2.5	0.48432 ± 0.00112	8078 ± 191	40.72 ± 0.20	50.63 ± 0.20
TT-3-Top ^e	61823	± 7	2292.0	± 5	73.5 ± 2.1	0.20259 ± 0.00043	9021 ± 25	22.78 ± 0.74	22.71 ± 0.74
TT-3-Bottom ^e	3582	± 15	61.0	± 7	91.5 ± 2.3	0.2638 ± 0.0018	254225 ± 28994	30.09 ± 0.25	30.03 ± 0.25
TT-5-Top ^e	5415	± 10	77.0	± 7.9	90.8 ± 2.0	0.26439 ± 0.00072	306510 ± 31642	30.15 ± 0.12	30.08 ± 0.12
TT-5-Bottom ^e	2112	± 3	57.6	± 7.7	86.3 ± 1.8	0.27268 ± 0.00075	164858 ± 22073	31.39 ± 0.12	31.32 ± 0.12

Note: Analytical errors are 2σ of the mean; $^a\delta^{234}\text{U} = ([^{234}\text{U}/^{238}\text{U}]_{\text{activity}} - 1) \times 1000$; $^b\delta^{234}\text{U}_{\text{initial}}$ corrected was calculated based on ^{230}Th age (T), i.e., $\delta^{234}\text{U}_{\text{initial}} = \delta^{234}\text{U}_{\text{measured}} \times e^{\lambda^{234}\text{T}}$, and T is corrected age; $^c[^{230}\text{Th}/^{238}\text{U}]_{\text{activity}} = 1 - e^{-\lambda^{230}\text{T}} + (\delta^{234}\text{U}_{\text{measured}}/1000)[\lambda_{230}/(\lambda_{230} - \lambda_{234})](1 - e^{-(\lambda_{230} - \lambda_{234})\text{T}})$, where T is the age; d Age corrections, relative to 1950 AD, were calculated using an estimated atomic $^{230}\text{Th}/^{232}\text{Th}$ ratio of $4 (\pm 2) \times 10^{-6}$. Those are the values for a material at secular equilibrium with the crustal $^{232}\text{Th}/^{238}\text{U}$ value of 3.8. The errors are arbitrarily assumed to be 50%; e The uranium and thorium isotopic compositions and ages data of TT-3 and TT-5 are from Nguyen et al. (2020; 2025)

Closed-system behavior, validated by Hendy tests (Hendy, 1971; Dorale et al., 1992), refers to the condition in which the speleothem remains geochemically isolated from post-depositional exchange with external fluids or gases. In such systems, the primary calcite/aragonite is dense and free from recrystallization, ensuring that its isotopic ($\delta^{18}\text{O}$, $\delta^{13}\text{C}$) and trace-element compositions reflect only the conditions of precipitation rather than later diagenetic alteration (Fairchild et al., 2006). This contrasts with the aragonite-to-calcite recrystallization problems reported in the surveyed cave in Ninh Binh province, where open-system behavior may have modified the original isotopic signal. The Hendy test results for NS3, HS3, TT-03, TT-05, and HS16 confirm that stalagmites collected in a closed system environment have

a high potential to be formed under equilibrium conditions. Furthermore, the combined Hendy test results and U/Th dating indicate that the stability of the growth conditions is closely linked to the stalagmite's equilibrium.

4.3. The potential time span and paleoclimate issues

U/Th dating further confirms the late Quaternary age of our specimens, with ages ranging from 19 ka (HS17-Top) to 129 ka (HS9b-Bottom) and errors mostly below 0.5% (Table 6, Fig. 8), and is supported by growth rates exceeding 0.09 mm/year. A composite record of TT-3 and TT-5 further confirmed monsoon-driven isotopic shifts, with overlapping growth intervals highlighting regional climate consistency (Chiang et al.,

2025). These findings underscore Thuong Thien's importance among Son La caves and support its potential as a paleomonsoon archive, in line with this study's broader survey results. However, HS7's non-equilibrium deposition ($R^2 = 0.74$, Fig. 7), despite identical humidity, suggests

environmental complexity, potentially driven by drip-rate variability or cave ventilation factors untested here but noted in karst studies (Fairchild et al., 2006). This contrast underscores the necessity of rigorous site selection and Hendy test validation to ensure proxy reliability.

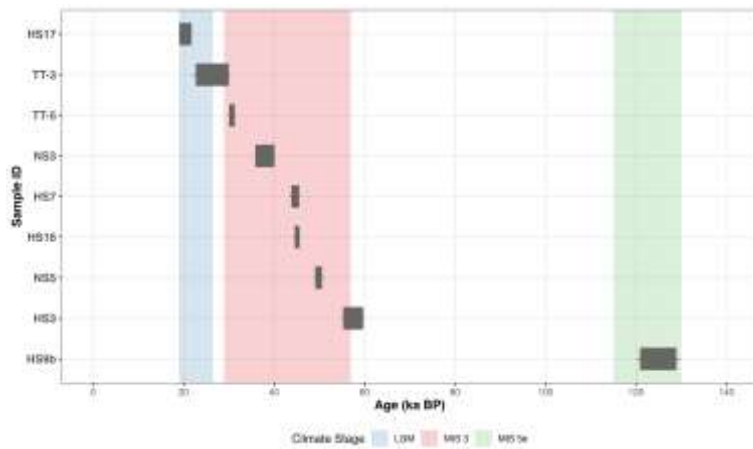


Figure 8. U/Th dating results with 2σ errors of Northern Vietnam stalagmites reported in this study

The scope of this study surveying 51 caves across seven provinces (Table 1) provides a more systematic foundation than previous efforts in Northern Vietnam, such as Nguyen et al. (2020), which focus on a single cave with decadal-resolution records linked to Dansgaard-Oeschger events 2–4. Our collection of 127 stalagmites, with detailed environmental data (e.g., humidity, cave type), extends the spatial coverage beyond that of earlier work. Hendy testing of 56 subsamples from four stalagmites, combined with U/Th dating of eight subsamples, establishes a robust methodological framework. For instance, the isotopic stability and precise age of stalagmite NS3 ($35,949 \pm 172$ yr BP, Table 6) contrast with Nguyen et al. (2022), who focused on Heinrich Event 3 from Thuong Thien cave, thereby providing a broader regional baseline. Compared with the extensive speleothem records from Southwest China (Dongge, Sanbao; Cheng et al., 2016), the stalagmites from Northern Vietnam form under comparable environmental conditions

near-saturated humidity and growth rates conducive to high-resolution paleoclimate reconstructions. Nevertheless, challenges such as the aragonite-to-calcite transformation in Khong cave (with 85% humidity) and the porosity of stalagmites collected in Hua Ma cave indicate greater depositional variability than observed in China's more homogeneous datasets. These observations underscore the necessity of site-specific assessment: low humidity (85% in Khong Cave) correlates with mineral instability, whereas high moisture (99.9% in Hoa Son) favors equilibrium deposition.

Preliminary isotopic data from NS3 suggest that $\delta^{18}\text{O}$ reflects monsoon rainfall and moisture source variability, consistent with regional monsoon signals (-6 to -8‰; Yang et al., 2016). In contrast, $\delta^{13}\text{C}$ may track vegetation shifts, aligning with karst studies that link carbon isotopes to surface conditions (Genty et al., 2003). The 1-sigma variations of coeval $\delta^{18}\text{O}$ data ranged in NS3 ($\pm 0.14\text{‰}$ to $\pm 0.16\text{‰}$), indicating stable deposition,

validated by Hendy test criteria ($R^2 < 0.24$). However, isotopic data are currently limited to NS3, with HS3 and HS16 awaiting analysis a constraint noted in our ongoing work. This dual-proxy potential remains provisional until broader sampling confirms consistency across the Hoa Binh site. The current framework, integrating a 51-cave survey with precise U/Th dating (HS16-Top: $42,751 \pm 180$ yr. BP, Table 6) and Hendy testing, establishes a methodological standard for speleothem research in Northern Vietnam. Our detailed analyses of four of the 127 stalagmites collected establish a proof-of-concept, surpassing the scale and rigor of prior studies (Nguyen et al., 2020, 2022) and identifying Hoa Binh and Lai Chau as prime locations for future isotopic campaigns.

Northern Vietnam's stalagmites, with growth rates and U/Th spans comparable to those in China (Table 6), offer a southern perspective to complement the northern records of the Asian monsoon. Positioned near the East Sea and influenced by ITCZ dynamics, this region enhances the spatial context of monsoon variability. The 35–59 ka range (HS7-Bottom: $52,639 \pm 231$ yr. BP, Table 6) falls within Marine Isotope Stage 3, a period of the Last Glacial Period, suggesting a potential to explore forcing mechanisms such as Heinrich Event 3 (Nguyen et al., 2022) or solar modulation (Chiang et al., 2025). For example, NS3's $\delta^{18}\text{O}$ variability hints at monsoon fluctuations, though the absence of a time series, due to limited subsampling, precludes event-specific correlations. This limitation, tied to the study's preliminary scope, underscores the need for ongoing isotopic analyses to build temporal resolution. By establishing a foundation rooted in extensive surveying (Table 1) and validated methods, this work positions Northern Vietnam as a key region for advancing Southeast Asian paleomonsoon research, with Hoa Binh stalagmites poised to unlock further climate insights.

5. Conclusions

The 51-cave survey and promising results from Hoa Binh position this region as a key frontier, complementing China's records with a southern perspective. Equilibrium deposition in NS3, HS3, and HS16, validated by Hendy tests on 56 subsamples and U/Th ages spanning 36–60 ka, confirms their potential for stable-isotopic analysis. The $\delta^{18}\text{O}$ 1-sigma variations ($\pm 0.04\text{--}0.20\text{\textperthousand}$) confirm equilibrium deposition for NS3, HS3, and HS16, making them reliable precipitation proxies, though broader applicability awaits further sampling. In contrast, HS7's non-equilibrium despite 99.9% humidity highlights depositional variability, reinforcing the Hendy test's role in site vetting. Furthermore, $\delta^{13}\text{C}$ variations ($\pm 0.04\text{--}0.71\text{\textperthousand}$) reveal substantial fractionation, likely due to degassing, necessitating careful analysis of $\delta^{13}\text{C}$ data for paleoclimate purposes. This framework, which integrates extensive surveying, precise U/Th dating (relative errors $< 0.5\%$), and Hendy testing, establishes a rigorous standard for Northern Vietnam and surpasses prior single-site studies. Positioned south of China's records, these stalagmites offer a complementary perspective on Asian Monsoon dynamics, with growth rates (> 0.09 mm/year) suggesting high-resolution potential for the future. Ongoing isotopic analyses will build on this foundation to explore glacial and deglacial forcing, thereby enhancing our understanding of Southeast Asia's paleoclimate.

Ideal stalagmites for future analyses should be clean, non-porous, exhibit clear growth rings, and demonstrate stable growth. While it is possible to collect non-porous stalagmites with clear growth rings, which may not be very clean and may exhibit unstable growth, we must evaluate these specimens with great care. Ultimately, our focus should be on identifying and collecting stalagmites that meet the criteria of cleanliness, non-porosity, and stable development to ensure the accuracy of our analysis.

Acknowledgements

A grant for the basic research project has supported this research (No. 105.99-2021.71) from the National Foundation for Science and Technology Development (Nafosted) of Vietnam to Nguyen Thuy Duong. The authors thank Prof. Horng-Sheng Mii for supporting the Hendy test analysis. U-Th dating in the HISPEC, NTU, was endorsed by the NSTC (111-2116-M-002-022-MY3, 113-2926-I-002-510-G to CCS), Higher Education Sprout Project of the Ministry of Education (112L894202 to CCS), and National Taiwan University Core Consortiums Project (113L891902 to CCS).

References

Beck H.E., Zimmermann N.E., McVicar T.R., Vergopolan N., Berg A., Wood E.F., 2018. Present and future Köppen-Geiger climate classification maps at 1 km resolution. *Sci Data*, 5, 180214. <https://doi.org/10.1038/sdata.2018.214>.

Cheng H., Edwards R.L., Sinha A., Spötl C., Yi L., Chen S., Kelly M., Kathayat G., Wang X., Li X., Kong X., Wang Y., Ning Y., Zhang H., 2016. The Asian monsoon over the past 640,000 years and ice age terminations. *Nature*, 534, 640–646. <https://doi.org/10.1038/nature18591>.

Cheng H., Lawrence Edwards R., Shen C.-C., Polyak V.J., Asmerom Y., Woodhead J., Hellstrom J., Wang Y., Kong X., Spötl C., Wang X., Calvin Alexander E., 2013. Improvements in ^{230}Th dating, ^{230}Th and ^{234}U half-life values, and U-Th isotopic measurements by multi-collector inductively coupled plasma mass spectrometry. *Earth and Planetary Science Letters*, 371–372, 82–91. <https://doi.org/10.1016/j.epsl.2013.04.006>.

Chiang H.-W., Chen Y.-G., Lee S.-Y., Nguyen D.C., Shen C.-C., Lin Y., Doan L.D., 2025. Speleothem evidence of solar modulation on the south Asia monsoon intensity. *npj Climate and Atmospheric Science*, 8, 105. <https://doi.org/10.1038/s41612-025-00971-8>.

Chiang H.W., Lu Y., Wang X., Lin K., Liu X., 2019. Optimizing MC-ICP-MS with SEM protocols for determination of U and Th isotope ratios and ^{230}Th ages in carbonates. *Quaternary Geochronology*, 50, 75–90. <https://doi.org/10.1016/j.quageo.2018.10.003>.

Chiang J.C.H., Kong W., Wu C.H., Battisti D.S., 2020. Origins of East Asian Summer Monsoon Seasonality. *Journal of Climate*, 33, 7945–7965. <https://doi.org/10.1175/JCLI-D-19-0888.1>.

Cruz F.W., Burns S.J., Karmann I., Sharp W.D., Vuille M., Cardoso A.O., Ferrari J.A., Silva Dias P.L., Viana O., 2005. Insolation-driven changes in atmospheric circulation over the past 116,000 years in subtropical Brazil. *Nature*, 434, 63–66. <https://doi.org/10.1038/nature03365>.

Dorale J.A., Edwards R.L., Calvin A.E.Jr., Shen, C.C., Richards D., Cheng H., 2007. Uranium-Series Dating Of Speleothemes: Current Techniques, Limits and Applications, Studies of Cave Sediments, 177–197. https://doi.org/10.1007/978-1-4419-9118-8_10.

Dorale J.A., González L.A., Reagan M.K., Pickett D.A., Murrell M.T., Baker R.G., 1992. A High-Resolution Record of Holocene Climate Change in Speleothem Calcite from Cold Water Cave, Northeast Iowa. *Science*, 258(5088), 1626–1630. <https://doi.org/10.1126/science.258.5088.1626>.

Dreybrodt W., Scholz D., 2011. Climatic dependence of stable carbon and oxygen isotope signals recorded in speleothems: From soil water to speleothem calcite. *Geochimica et Cosmochimica Acta*, 75, 734–752. <https://doi.org/10.1016/j.gca.2010.11.002>.

Dykoski C., Edwards R., Cheng H., Yuan D., Cai Y., Zhang M., Lin Y., Qing J., An Z., Revenaugh J., 2005. A high-resolution, absolute-dated Holocene and deglacial Asian monsoon record from Dongge Cave, China. *Earth and Planetary Science Letters*, 233, 71–86. <https://doi.org/10.1016/j.epsl.2005.01.036>.

Edwards R.L., Chen J.H., Wasserburg G.J., 1987. ^{238}U - ^{234}U - ^{230}Th systematics and the precise measurement of time over the past 500,000 years. *Earth and Planetary Science Letters*, 81, 175–192. [https://doi.org/10.1016/0012-821X\(87\)90154-3](https://doi.org/10.1016/0012-821X(87)90154-3).

Fairchild I.J., Smith C.L., Baker A., Fuller L., Spötl C., Matthey D., McDermott F., E.I.M.F.,

2006. Modification and preservation of environmental signals in speleothems. *Earth-Science Reviews*, 75, 105–153. <https://doi.org/10.1016/j.earscirev.2005.08.003>.

Fairchild I.J., Baker A., 2012. Speleothem science: from process to past environments. John Wiley & Sons. <https://doi.org/10.1002/9781444361094>.

Ford D., Williams P.W. (Eds.), 2010. Karst hydrogeology and geomorphology, Rev. ed. ed. John Wiley & Sons, Chichester, England A Hoboken, NJ.

Frisia, Silvia, 2015. Microstratigraphic logging of calcite fabrics in speleothems as tool for palaeoclimate studies. *International Journal of Speleology*, 44, 1–16. <http://dx.doi.org/10.5038/1827-806X.44.1.1>.

Genty D., Blamart D., Ouahdi R., Gilmour M., Baker A., Jouzel J., Van-Exter S., 2003. Precise dating of Dansgaard-Oeschger climate oscillations in western Europe from stalagmite data. *Nature*, 421, 833–837. <https://doi.org/10.1038/nature01391>.

Hanebuth T.J., Saito Y., Tanabe S., Vu Q.L., Ngo Q.T., 2006. Sea levels during late marine isotope stage 3 (or older?) reported from the Red River delta (northern Vietnam) and adjacent regions. *Quaternary International*, 145, 119–134. <https://doi.org/10.1016/j.quaint.2005.07.008>.

Henderson G.M., 2006. Caving In to New Chronologies. *Science*, 313, 620–622. <https://doi.org/10.1126/science.1128980>.

Hendy C.H., 1971. The isotopic geochemistry of speleothems I. The calculation of the effects of different modes of formation on the isotopic composition of speleothems and their applicability as palaeoclimatic indicators. *Geochimica et Cosmochimica Acta*, 35, 801–824. [https://doi.org/10.1016/0016-7037\(71\)90127-X](https://doi.org/10.1016/0016-7037(71)90127-X).

Hu H.-M., Shen C.-C., Cheng H., Woodhead J., Edwards R.L., Zhao J.-X., Huang C.-Y., Lu P.-Y., Chien W.-Y., Wang J., Jia X., Yokoyama Y., Cai Y., Zachariáš J., 2025. Sub-epsilon natural $^{234}\text{U}/^{238}\text{U}$ measurements refine the ^{234}U half-life and the U-Th geochronology. *Science Advances*, 11, eadu8117. <https://www.science.org/doi/10.1126/sciadv.adu8117>.

Jaffey A.H., Flynn K.F., Glendenin L.E., Bentley W.C., Essling A.M., 1971. Precision Measurement of Half-Lives and Specific Activities of ^{235}U and ^{238}U . *Physical Review C*, 4(5), 1889. <https://doi.org/10.1103/PhysRevC.4.1889>.

Labonne M., Hillaire-Marcel C., Ghaleb B., Goy J.-L., 2002. Multi-isotopic age assessment of dirty speleothem calcite: an example from Altamira Cave, Spain. *Quaternary Science Reviews*, 21, 1099–1110. [https://doi.org/10.1016/S0277-3791\(01\)00076-2](https://doi.org/10.1016/S0277-3791(01)00076-2).

Lachniet M.S., 2009. Climatic and environmental controls on speleothem oxygen-isotope values. *Quaternary Science Reviews*, 28, 412–432. <https://doi.org/10.1016/j.quascirev.2008.10.021>.

Markowska M., Baker A., Andersen M.S., Jex C.N., Cuthbert M.O., Rau G.C., Graham P.W., Rutledge H., Mariethoz G., Marjo C.E., Treble P.C., Edwards N., 2016. Semi-arid zone caves: Evaporation and hydrological controls on $\delta^{18}\text{O}$ drip water composition and implications for speleothem paleoclimate reconstructions. *Quaternary Science Reviews*, 131, 285–301.

McDermott F., 2004. Palaeo-climate reconstruction from stable isotope variations in speleothems: a review. *Quaternary Science Reviews*, 23, 901–918. <https://doi.org/10.1016/j.quascirev.2003.06.021>.

Mickler P.J., Stern L.A., Banner J.L., 2006. Large kinetic isotope effects in modern speleothems. *GSA Bulletin*, 118, 65–81. <https://doi.org/10.1130/B25698.1>.

Mühlinghaus C., Scholz D., Mangini A., 2009. Modelling fractionation of stable isotopes in stalagmites. *Geochimica et Cosmochimica Acta*, 73, 7275–7289. <https://doi.org/10.1016/j.gca.2009.09.010>.

Nguyen D.C., Chen Y.-G., Chiang H.-W., Shen C.-C., Wang X., Doan L.D., Yuan S., Ahmad Lone M., Yu T.-L., Lin Y., Kuo Y.-T., 2020. A decadal-resolution stalagmite record of strong Asian summer monsoon from northwestern Vietnam over the Dansgaard–Oeschger events 2–4. *Journal of Asian Earth Sciences*, X(3), 100027. <https://doi.org/10.1016/j.jaesx.2020.100027>.

Nguyen D.C., Lee S.-Y., Chen Y.-G., Chiang H.-W., Shen C.-C., Wang X., Doan L.D., Lin

Y., 2022. Precipitation response to Heinrich Event-3 in the northern Indochina as revealed in a high-resolution speleothem record. *Journal of Asian Earth Sciences*, X(7), 100090. <https://doi.org/10.1016/j.jaesx.2022.100090>.

Nguyen D.N., Nguyen T.H., 2004. Vietnam climate and climate resources. Publishing house for Agriculture, Hanoi (in Vietnamese).

Phan C.T. (Editor-in-Chief), Le D.A., Le D.B., Dao D.B., Bosaykham V., Bounthong P., Tran D., Nguyen D.D., Hoang T.D., Tran Q.H., Vu K., Som C.K., Pham D.L., Mai N.L., Nguyen Q.M., Phung K.N., Nguyen N., Nouphet R., Nguyen K.Q., Nguyen V.Q., Saykham D.A., Ton D.T., T.V.T., Truyen M.T., Xay T.S., 1991. Geological map of Cambodia, Laos and Viet Nam on 1:1.000.000. Vietnam Institute of Geosciences and Mineral Resources (in Vietnamese).

Sánchez-Moreno E.M., Font E., Pavón-Carrasco F.J., Dimuccio L.A., Hillaire-Marcel C., Ghaleb B., Cunha L., 2022. Paleomagnetic techniques can date speleothems with high concentrations of detrital material. *Scientific Reports*, 12, 17936. <https://doi.org/10.1038/s41598-022-21761-9>.

Scholz D., Hoffmann D.L., 2011. StalAge - An algorithm designed for construction of speleothem age models. *Quaternary Geochronology*, 6, 369–382. <https://doi.org/10.1016/j.quageo.2011.02.002>.

Shen C.C., Lawrence E.R., Cheng H., Dorale J.A., Thomas R.B., Bradley M.S., Weinstein S.E., Edmonds H.N., 2002. Uranium and thorium isotopic and concentration measurements by magnetic sector inductively coupled plasma mass spectrometry. *Chemical Geology*, 185, 165–178. [https://doi.org/10.1016/S0009-2541\(01\)00404-1](https://doi.org/10.1016/S0009-2541(01)00404-1).

Shen C.-C., Wu C.-C., Cheng H., Lawrence Edwards R., Hsieh Y.-T., Gallet S., Chang C.-C., Li T.-Y., Lam D.D., Kano A., Hori M., Spötl C., 2012. High-precision and high-resolution carbonate ^{230}Th dating by MC-ICP-MS with SEM protocols. *Geochimica et Cosmochimica Acta*, 99, 71–86. <https://doi.org/10.1016/j.gca.2012.09.018>.

Sinha A., Cannariato K.G., Stott L.D., Li H.-C., You C.-F., Cheng H., Edwards R.L., Singh I.B., 2005. Variability of Southwest Indian summer monsoon precipitation during the Bølling-Ållerød. *Geology*, 33, 813–816. <https://doi.org/10.1130/G21498.1>.

Sterling E.J., 2006. Vietnam: A Natural History. Yale University Press, New Haven. <https://doi.org/10.12987/9780300128215>.

The Department of Geology and Minerals of Vietnam, 2005. The Geological and minerals map of Vietnam on 1:200.000 (in Vietnamese).

Tran V.T., 2009. Geology and Resources of Vietnam. Publishing House for Science and Technology (in Vietnamese).

University of East Anglia Climatic Research Unit, Harris I.C., Jones P.D., Osborn T., 2024. CRU CY4.08: Climatic Research Unit year-by-year variation of selected climate variables by country version 4.08 (Jan. 1901 - Dec. 2023). NERC EDS Centre for Environmental Data Analysis, date of citation. <https://catalogue.ceda.ac.uk/uuid/3b7f475a30a642e9af5323cef748bb00/>.

van Oldenborgh G.J., 2020. KNMI Climate Explorer [WWW Document]. URL. <https://climexp.knmi.nl/start.cgi>. (Accessed 18 March 2025).

Wolf A., Ersek V., Braun T., French A.D., McGee D., Bernasconi S.M., Skiba V., Griffiths M.L., Johnson K.R., Fohlmeister J., Breitenbach S.F.M., Pausata F.S.R., Tabor C.R., Longman J., Roberts W.H.G., Chandan D., Peltier W.R., Salzmann U., Limbert D., Trinh H.Q., Trinh A.D., 2023. Deciphering local and regional hydroclimate resolves contradicting evidence on the Asian monsoon evolution. *Nat Commun*, 14, 5697. <https://doi.org/10.1038/s41467-023-41373-9>.

Wortham B.E., Banner J.L., James E.W., Edwards R.L., Loewy S., 2022. Application of cave monitoring to constrain the value and source of detrital $^{230}\text{Th}/^{232}\text{Th}$ in speleothem calcite: Implications for U-series geochronology of speleothems. *Palaeogeography, Palaeoclimatology, Palaeoecology*, 596, 110978. <https://doi.org/10.1016/j.palaeo.2022.110978>.

Yang H., Johnson K.R., Griffiths M.L., Yoshimura K., 2016. Interannual controls on oxygen isotope variability in Asian monsoon precipitation and implications for paleoclimate reconstructions. *JGR Atmospheres*, 121, 8410–8428. <https://doi.org/10.1002/2015JD024683>.